A Soft, Wearable Skin-Brace for Assisting Forearm Pronation and Supination With a Low-Profile Design

Huimin Su, Kyoung-Soub Lee, Yusung Kim, and Hyung-Soon Park

***Abstract*—Neurological diseases affect more than 50 million people living with persistent upper limb impairments worldwide, and 40% of patients remain impaired even after intensive hospital care. Wearable robots have been developed for enhancing functionality in activities of daily living (ADL). The role of forearm movement is as crucial as the hand and wrist. However, the coincidence of the rotation axis with the forearm presents design challenges, and thus there are few studies on wearable devices for assisting forearm pronation/supination movement. In this study, we propose a bioinspired soft wearable skin-brace for the forearm pronation/supination to assist patients in ADL and perform rehabilitation training. The low-profile design that can fit the forearm like clothing combines features of a rail structure and tendon driving mechanism with high transfer efficiency. We conducted a biomechanical analysis to quantify the movement of wrist landmarks during forearm rotation, as well as a performance evaluation and user tests with our prototype. We demonstrate that it can provide patients with sufficient and compliant support in terms of range of motion and output torque. The user-friendly design allows patients to don and doff the device independently and quickly, as well as for individual customization. With the advantage of not restricting other joint movements, the device also shows the possibility of co-use with other rehabilitation devices.**

***Index Terms*—Prosthetics and exoskeletons, rehabilitation robotics, tendon/wire mechanism, wearable robotics.**

I. Introduction

NEUROLOGICAL diseases, such as stroke, and spinal cord injury (SCI), affect more than 50 million people living with persistent upper limb impairments worldwide [1]. In activities of daily living (ADL) involving upper limb movement, the role of forearm movement is crucial. For example, most upper limb movements such as drinking water, using utensils, and opening doors require the synergy of forearm pronation/supination movement. Unfortunately, patients suffering from neurological diseases experience forearm spasticity, which restricts them from conducting ADL tasks. Consequently, their quality of life drops drastically.

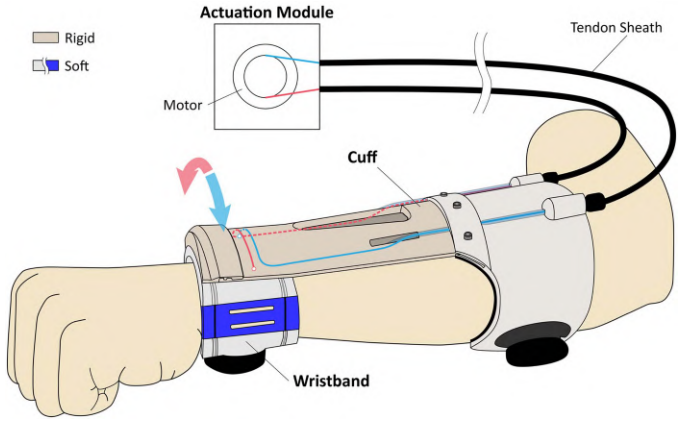

Fig. 1. Schematic of the wrist-forearm skin-brace. The device consists of a wristband module, a cuff module, and a remote actuation module connected to the cuff module via tendon sheaths. The design combines both features of a compact guide-rail structure and soft mechanism. The blue and red lines represent the tendon activating forearm supination and pronation, respectively. Both cables are driven by one motor at each rotational direction.

To help patients overcome this predicament, robot-assisted rehabilitation has drawn much interest in the last decade [2]. Usually, patients must undergo typical treatments such as physical therapy and occupational therapy in rehabilitation centers for several weeks or even months. Robot-assisted rehabilitation enables patients to conduct their own rehabilitation training while reducing the workload of therapists.

Recently, the portability of rehabilitation robots has received attention due to many patient with no or limited access to rehabilitation hospitals or centers for treatment under the global pandemic of COVID-19 [3]. Therefore, for rehabilitation training beyond the confines of professional large facilities, more rehabilitation resources must be moved to a community setting and even patients' homes to complement conventional therapy [4]. While portability and simplicity are key features of home-based personalized rehabilitation devices, state-of-the-art robot-assisted forearm pronation/supination rehabilitation devices have implemented pronation/supination by constructing a guide rail around the forearm, driven by a motor placed on the periphery of the rail [5], [6]; however, it is difficult to achieve a light and compact design.

Meanwhile, more stringent requirements should be applied to the compatibility of rehabilitation devices for patients. Impaired upper extremity function in stroke survivors usually involves more than a single degree of freedom (DOF) [7] and forearm

Manuscript received 17 May 2022; accepted 22 September 2022. Date of publication 4 October 2022; date of current version 13 October 2022. This letter was recommended for publication by Associate Editor A. L. Trejos and Editor J.-H. Ryu upon evaluation of the reviewers' comments. This work was supported by the National Research Foundation of Korea (NRF) Funded by the Korea Government (MSIT) under Grant NRF-2020R1A2C2012641. *(Corresponding author: Hyung-Soon Park.)*

The authors are with the Department of Mechanical Engineering, Korea Advanced Institute of Science and Technology, Daejeon 34141, South Korea (e-mail: suhuimin@kaist.ac.kr; lks0872@kaist.ac.kr; fjfrom92@kaist.ac.kr; hyungspark@kaist.ac.kr).

This work involved human subjects or animals in its research. Approval of all ethical and experimental procedures and protocols was granted by Korea Advanced Institute of Science and Technology Institutional Review Board under Application No. KH2020-185.

This letter has supplementary downloadable material available at https://doi.org/10.1109/LRA.2022.3211783, provided by the authors.

Digital Object Identifier 10.1109/LRA.2022.3211783

pronation/supination is as important as other DOFs of the upper limb. Existing forearm rehabilitation devices [5], [6] mostly require the patient to grasp a handle to fix the wrist (distal forearm) position, and cannot be used simultaneously with other rehabilitation devices such as hand devices. Furthermore, despite various forms of rehabilitation efforts, 40% of stroke survivors remain impaired even after training [8]. Their remaining capabilities are not expected to be further improved. For these patients, a lightweight wearable device would help them to perform ADL. Compared to previous research [9], [10], [11], [12] on the hand and wrist in recent years, there are few studies focusing on wearable devices specifically designed for forearm pronation/supination [13].

As a solution to these challenges, this study presents a design and subsequent evaluation of a wearable skin-brace (Fig. 1) to improve patient ADL as well as perform rehabilitation training tasks. The combined design of a compact rail structure and a soft tension transfer mechanism achieve light weight and compact skin-brace for forearm pronation/supination without restricting other joint movements for compatibility. In addition, the letter introduces design method for personalized usability based on the individualized biomechanical analysis for efficient and comfortable use.

II. Mechanism Design

A. Design Requirements

Forearm pronation/supination occurs as the radius rotates around the ulna along an axis from the head of the radius through the fovea of the distal ulna to rotate the wrist to perform functional tasks [14]. The pronator teres and pronator quadratus are the major muscles of forearm pronation, whereas the supinator and biceps brachii are the major muscles of supination [15]. Fig. 2(a)–(c) show the forearm anatomy and muscle actions of pronation/supination.

The mechanism design for forearm pronation/supination movement in an exoskeleton is challenging. Since its rotation axis coincides with the forearm, which is a fairly unique case and different from most joint movements, the existing devices adopt designs using a rail around the forearm [5], [6]. For compact design, a tendon driven mechanism has been introduced [11]. For efficient force transmission and for avoiding unnecessary joint and skin pressure, the tension force should make a pure moment in forearm rotation direction. It is difficult to route the tendon with minimized rigid constraints to create a pure rotational moment around the forearm while not occupying large space. In summary, we aim to provide a robotic device for forearm pronation/supination which is compact, lightweight, comfortable, and efficient.

The proposed device ultimately aims to provide suitable assistance to patients with functional impairment in forearm pronation/supination. We derived detailed requirements from previous studies and previous prototypes, summarized in Table I. For the forearm pronation/supination movement, a range of motion (ROM) of 150° is required along with a torque of 60 mNm to perform basic ADL [16].

In addition to ensuring sufficient physical performance to assist daily activities, other design features such as weight, size, and ease of donning/doffing are essential to enhance the daily usability of the device. Subjects with hand impairment expressed that wearing a device heavier than 500 g on the forearm was uncomfortable, and anything thicker than 30 mm was considered bulky [17]. In an unsupervised operating environment, simplicity is paramount [18]. Fast and independent donning and doffing of the device within 2 minutes is considered acceptable [10], [19]. Furthermore, factors such as comfort, ergonomics, individual customization, and compatibility with other DOFs should also be addressed.

TABLE I
Requirements for a Wearable Forearm Exoskeleton Design

Requirement	Values	Reference
Range of motion	150°	[6], [17]
Output torque	60mNm	[6], [17]
Weight	500g	[18]
Size (Thickness)	30mm	[18]
Donning/Doffing time	120s	[13], [20]
Further factors	Comfort, ergonomics, individual customization, no restriction on other DOFs	

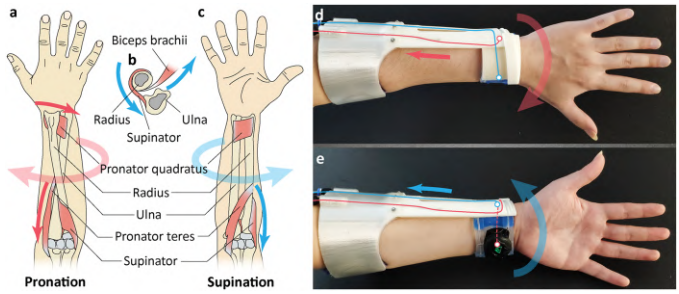

Fig. 2. Bioinspired mechanism based on the musculoskeletal characteristics of pronation/supination. (a) Anatomy of forearm pronation movement: pronator teres and pronator quadratus are the major contributing muscles. (b) and (c) Anatomy of forearm supination movement: supinator and biceps brachii are the major contributing muscles. (d) Pronation movement driven by the tendon mechanism in the skin-brace (e) Supination movement driven by the tendon mechanism in the skin-brace.

B. Design of the Skin-Brace

Inspired by forearm kinematic anatomy, we designed an elegant approach for assisting the forearm pronation/supination movement based on a customized compact rail-tendon actuating mechanism that mimics the pronator quadratus and pronator teres muscle-tendon model of the forearm (Fig. 2(a)). For a low-profile design, we chose the tendon drive as the transmission approach and the actuator was remotely placed outside of the forearm to reduce the inertia of the device worn at the forearm. We adopted a hybrid structure design that combines both soft and rigid mechanisms to impose constraint on tendon routing to avoid unnecessary pressure on the joint and skin, as well as improve transmission efficiency.

The proposed skin-brace (Fig. 1) consists of three parts: 1) a wristband, 2) a cuff, and 3) an actuation module. Guided by the rail on the cuff and the slider on the wristband, two cables are connected to the remote actuation system from the anchor points fixed on the wristband via the Teflon tubes on the cuff and the tendon sheath. Therefore, the device can assist pronation/supination (Fig. 2(d) and (e)) of the forearm by driving the wrist to rotate along with the wristband.

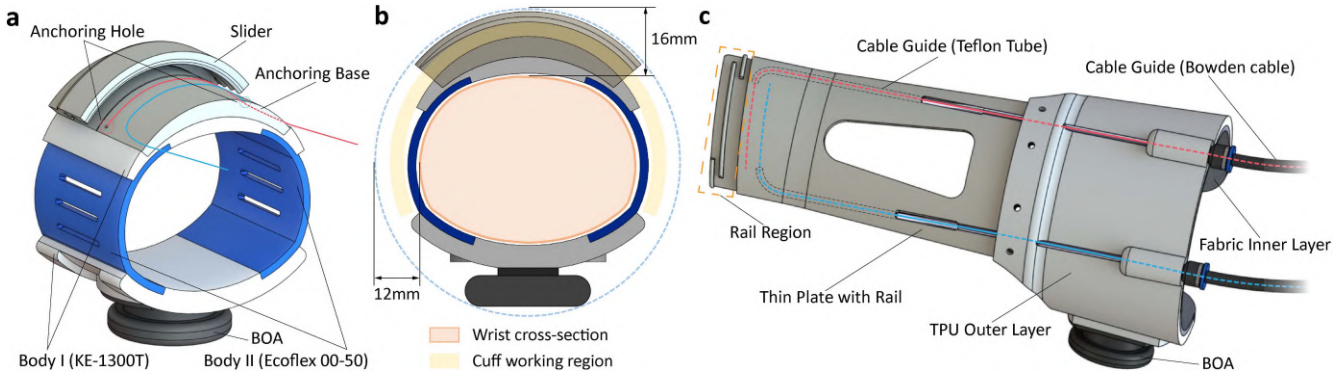

Fig. 3. Mechanical design of the wrist-forearm Module. (a) Wristband design (mobile): The cables attached to the anchoring base of the wrist band makes pronation/supination movement guided by the slider which is a part of the compact guided-rail mechanism. (b) Dimension of the wristband: Soft stretchable silicon and BOA allow tight and comfortable fit. (c) Cuff design: The rail is integrated at the distal end of the thin plate. In (a) and (c), the blue and red lines represent the tendon activating forearm supination and pronation, respectively.

1) Wristband: The body of the wristband (Fig. 3(a)) is made of KE-1300 T (Shin-Etsu, Japan) and Ecoflex 00–50 (Smooth-on, US): two types of silicone material with different elongation and hardness. The combination of the silicon materials increases the friction to ensure a firm fixation to the wrist, even at low pressure, and alleviates the discomfort caused by prolonged wearing. The slider and anchoring base for anchoring cables are 3D printed from ABS material to resist deformation of the wristband caused by cable tension. A Teflon coating is added to the surface of the anchoring base to reduce the friction caused by the rotation between the wristband and cuff. Two cables are fixed at both sides of the anchoring base and fed into the Teflon tubes on the cuff. To simplify the steps of wearing and improve its fastening quality, we adopted the BOA lacing system to achieve radial flexibility and ensure the integration of the wristband.

To provide users with a compact wristband, we optimized the design of the wristband based on the wrist ratio: the ratio of wrist depth to wrist width. For human wrists, the value is about 0.6 [20], [21]; thus, we designed the inner shape of the wristband as a near-elliptical shape based on this parameter and constructed a feasible slider with a small radius to minimize the overall dimension of the wristband. By thoughtful calculation of the spatial geometry around the wrist, there are no unnecessary clearances when the wristband and cuff are sliding against each other (Fig. 3(b)). The thickest part of the wristband is only 16 mm, and the diameter of its overall working area is merely 12 mm wider than the wrist width.

2) Cuff: The cuff (Fig. 3(c)) serves two primary functions. The first is to fix the rail to ensure that the relative position of the rail and the proximal end of the forearm remain static when the slider rotates on the rail. Secondly, it can provide axial support to prevent distortion caused by cable tension and strictly restricts the tendon routes. The distal end of the cuff is a thin plate made of ABS integrated with a rail and grooves for the tendon routes. The Teflon tubes guide the cable with low friction and are embedded in the grooves of the plate. The proximal end of the cuff consists of two layers. The material of the outer layer is TPU, which is flexible while providing sufficient stiffness to the brace. The inner layer is composed of tailored fabric for a comfortable wearing experience. The BOA system and elastic belts are also adopted for fast and easy donning and doffing.

This compact guide rail mechanism allows the wristband (slider) to partially pass through the rail to achieve a 150° rotation. The rail part is composed of three mutually misaligned tracks (Fig. 3(b)), which are matched in three independent grooves in the slider. Barriers are set up on different sides of the grooves to prevent the slider beyond the ROM. The longest track in the middle is set up for alignment, ensuring that both end of the slider can precisely return to the two shorter tracks after crossing them.

3) Bio-Adaptive Rail: For the exoskeleton design, since a misalignment between the exoskeleton and the limbs can have severe repercussions on long-term usage of these devices, the axes of rotation of the robot in the exoskeleton must match the axes of anatomical rotation of the user [22]. In our early pilot test, we found that a guide rail with a circular arc design would generate large, unexpected friction during movement. During the test, healthy participants were asked to voluntarily rotate their forearms while wearing the device. They reported obvious obstacles in performing this movement. We speculated that the circular arc rail does not adequately match the actual wrist rotation trajectory in forearm pronation/supination.

To determine the rotation trajectory of the wrist and verify our hypothesis, we adopted a 3D motion-capture system (Vicon, Oxford, U.K.) to measure the kinematic motion of the forearm. We attached seven reflective markers to the participants, three of which were on the wrist and distributed in the area where the rail was placed. The other four were attached to the proximal end of the forearm as reference points to establish the relative coordinate system (Fig. 4(a)). The Z axis is along the direction of the forearm, and the plane where the X and Y axis are located is perpendicular to the forearm. Then, the participants were instructed to perform the forearm pronation/supination motion from a neutral position. Throughout the test, their upper arm was immobilized and their elbow flexed at 90°.

By analyzing the measured motion capture data, we found that the trajectory of the markers on the wrist approximates a circular arc in the X-Y plane (Fig. 4(b)). In the X-Z plane, the trajectory of the markers on the wrist had a slight offset in the Z-axis direction, instead of a straight trajectory parallel to the X-axis (Fig. 4(c)). The offset was 8.93 ± 3.76 mm. Based on this result, we designed the shape of the rail as a section of the spiral structure to adapt to the kinematic motion of the human forearm (Fig. 4(e)). This mechanism enables the slider to complete a 150° rotation under the constraint of a 100° rail without occupying large space (Fig. 4(d) and (e)).

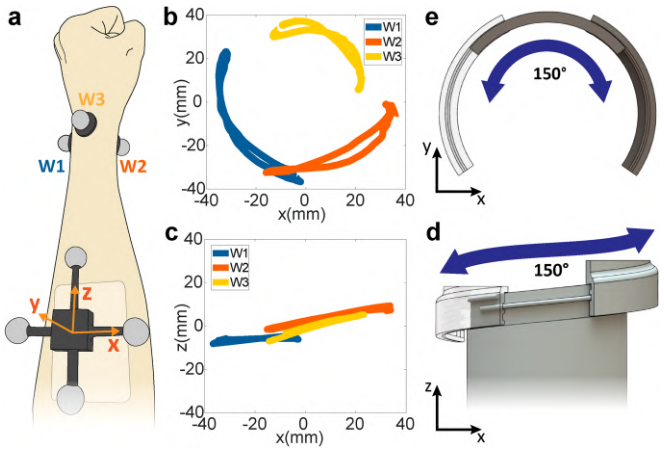

Fig. 4. Bio-adaptive rail design based on wrist rotation trajectory of pronation/supination. (a) Reflective marker attachment and reference coordinate setup. (b) Representative wrist rotation trajectory of pronation/supination in the X-Y plane (left arm). The trajectory is approximate to a circular arc. (c) Representative wrist rotation trajectory of pronation/supination in the X-Z plane (left arm). (d) Front view of the bio-adaptive rail design (e) Top view of the bio-adaptive rail design.

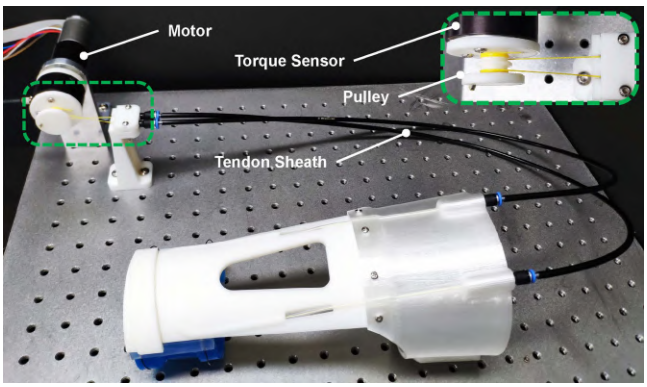

Fig. 5. Actuation system setup for evaluating the skin-brace. The green dashed area presents the connection of the tendons to the pulley, two tendons wound in opposite directions on the pulley.

4) Actuation Module: To miniaturize the actuation system, a pair of biomimetic antagonistic cables was attached to one pulley for bidirectional tensioning by a single motor. A critical challenge in tendon-driven mechanism is that the overall length of the tendon routes varies depending on the joint angle [9], which makes it difficult to implement the pull-pull tendon-driven mechanism with a single motor. Based on the proposed rail-tendon actuating mechanism, the tendon routes of the skin-brace can be accurately determined and strictly restricted. Therefore, the length changes of the two cables are kept complementary regardless of changes in forearm rotation angle, enabling to maintain a relatively constant path length, minimizing slack, which is a solid foundation for further implementing a portable actuation system.

For the proposed device, the current actuation unit is over the required specification and connected to the test bench to evaluate the characteristics and performance of the skin-brace (Fig. 5), consisting of an EC motor (EC i 30, maxon, Switzerland) with an encoder and a reduction ratio of 33:1, connected to a torque sensor (TRT-100, Transducer Techniques, US) to measure the output torque from the motor. Two microfilament braided wires (0.46 mm, PowerPro, USA) wound in opposite directions on the pulley (radius 6 mm) are connected to the anchoring base on the wristband via tendon sheath (5 mm, BBB Cycling, Netherlands) and Teflon tubes on the cuff. The control system for the brace adopted speed feedback control and operated at 1 kHz. The maximum output torque from the drive was limited by torque feedback to prevent potential injury to the user. Since a previous study has shown that a speed of 0.5 Hz during rehabilitation can induce cortical activation to enhance the rehabilitative effect [23], we restricted the maximum speed to 150°/s with limited acceleration.

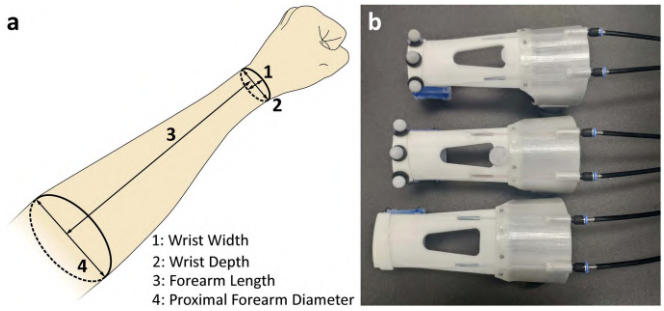

Fig. 6. Dimension Parameters Used for Creating User-customized 3D Brace Design. (a) Illustration of the forearm model with anthropometric parameters. (b) Three braces customized for subjects with different size.

C. Individual Customization

The forearm size and residual capacity of each individual user are different. In particular, patients with neurological diseases may have greater differences in body size due to tissue wasting [24]. To provide optimal support and a comfortable wearable experience for the user, we built a parameter-correlated modeling algorithm based on individual forearm anthropometric parameters (Fig. 6(a)).

We created the computer aided design (CAD) models of all 13 parts based on the wrist width, wrist depth, forearm length, and proximal forearm diameter of a user. By measuring and feeding user's forearm dimensions (Fig. 6(a)) into CAD models, all customized 3D parts of the skin-brace can be reconstructed by strict geometric constraints. Since most components of the brace are based on 3D printing prototyping technology, we were able to provide personalized braces to users with rapid and low-cost manufacturing. We fabricated three braces of different sizes (Fig. 6(b)) and the average weight of the braces is 133 g. Moreover, we can expand customization in the future by considering personal preferences like colors, materials, etc.

III. Experimental Validation

A. Output Torque and Efficiency Test

To evaluate the maximal output torque of the device, we constructed a dummy forearm-wrist model with humanlike dimensions (Fig. 7(a)). It includes a wrist model with a 6-axis force/torque sensor (Mini 45, ATI, US) to measure the output torque and a forearm proximal model. The cable tension is generated by the actuation unit. Six wrist models were made to match different forearm rotation angles (Fig. 7(b)).

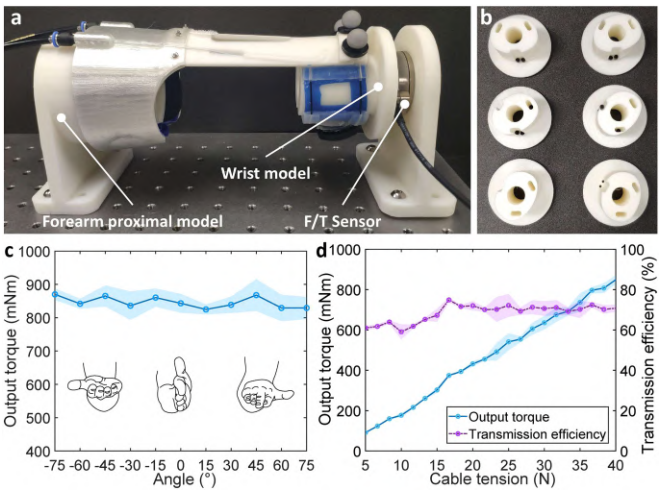

Fig. 7. Output torque and transmission efficiency of the device. (a) Experimental setup for the evaluation. (b) Wrist models for matching different forearm rotation angles. (c) Output torque at different angles with 40 N of cable tension. (d) Output torque and transmission efficiency with respect to the cable tension (operating range: 5 N∼40 N). In (c) and (d), the lines indicate the mean and the shaded area indicates the standard deviation.

We measured the output torque under 40 N cable tension for angles from $-75°$ to $75°$ (Fig. 7(c)). At each angle, the output torque remained relatively comparable, with a maximum output torque of 846.05 ± 33.27 mNm and no singularity of insufficient power. We also measured the output torque and the transmission efficiency at different input cable tensions (Fig. 7(d)). The minimum cable tension required to activate the device is approximately 5 N. When the cable tension was below this value, no obvious output torque was observed due to mechanical resistance. After conversion, the overall transmission efficiency of the device was $70.98\% \pm 5.15\%$.

B. User Test

1) Test Purpose and Participants: The performance and usability of the skin-brace was evaluated via four experiments. The first and second experiments focused on comparing the ROM and output torque of the forearm pronation/supination in the voluntary and device-assisted condition. The third experiment assessed the task performance improvement in ADL tasks. The last experiment focused on evaluating the wearability of the device by a donning/doffing test. All the participants were required to fill out questionnaires both before and after the experiments to evaluate the participants' physical condition and subjective impression of the skin-brace.

Six healthy participants (2 females and 4 males, all right-hand dominant, mean age: 27 ± 4.1) and three severe stroke survivors (2 females and 1 male, mean age: 60 ± 8.5) were recruited to participate in this experiment. The impairment severity of the stroke survivors was evaluated based on the Fugl-Meyer Assessment scale for Upper Extremity (FMA-UE) (demographics listed in Table II). Written informed consent was obtained from each participant prior to participation.

2) Experimental Setup and Protocol: Based on the parameter-correlated modeling algorithm and 3D printing rapid prototyping technology, we built a total of three braces of different sizes for participants, supporting both left and right arms (Fig. 6(b)). Similar to the trajectory determination test, we attached six reflective markers to the participants and three markers on the base. A 3D motion-capture system (Vicon, Oxford, U.K.) was applied to measure the ROM. Their shoulder abduction angles were 45° and their elbow flexed at 90°.

TABLE II
STROKE SURVIVORS DEMOGRAPHICS

No.	Gender	Age (Years)	Time since stroke (Years)	Affected side	FMA-UE Score (Max 36)
S1	F	52	7	Right	2
S2	F	69	21	Left	11
S3	M	59	7	Right	16

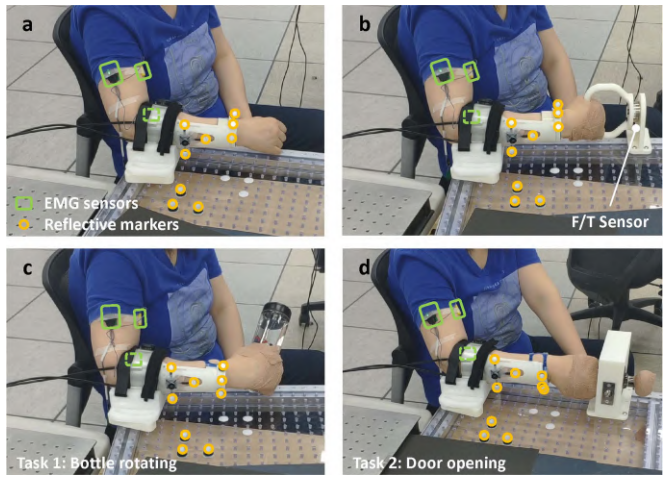

Fig. 8. Experimental setup for the usability test. (a) ROM test under assisted condition (Participant S2). (b) Output torque evaluation test (Participant S2). (c) Bottle rotating task (Participant S2). (d) Door opening task (Participant S2). The EMG sensors were attached to the pronator teres and biceps brachii for monitoring purposes.

To detect whether the participants were exerting volitional control of the forearm during the experiments, we attached electromyographic (EMG) sensors (Trigno Quattro, Delsys, US) on the pronator teres and biceps brachii to measure the muscle activation (Fig. 8(a)). The EMG signal was sampled at 2000 Hz and bandpass filtered using a Butterworth filter (30–450 Hz). We applied a 60 Hz notch filter to reduce the electric noise. The maximum voluntary contraction (MVC) was recorded as a reference standard. The output torque from the participants was measured by a force/torque sensor (Mini 45, ATI, US) which was mounted on the handle (Fig. 8(b)).

We compared the forearm ability of participants between voluntary and device assistance in terms of ROM. The participants were instructed to voluntarily perform a forearm pronation/supination motion from a neutral position. Then, with the device's assistance, all participants were required to relax their wrist and forearm naturally, and to passively complete the same task under the control of the device.

To compare the muscle effort and output torque between using and without using the device, we conducted isometric rotation experiments. The participants' hand was tied to a handle by a medical elastic bandage to avoid EMG signal crosstalk caused by a grasping force (Fig. 8(b)).

Among the various ADL tasks, two ADL tasks (Fig. 8(c) and (d)) that heavily involves the forearm pronation/supination were

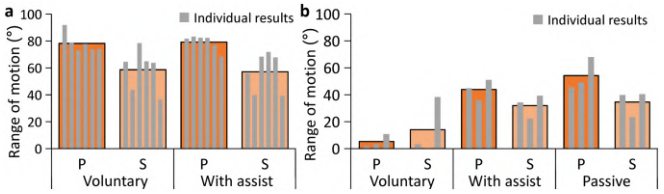

Fig. 9. ROM evaluation (a) ROM comparison of pronation/supination of healthy participants. (b) ROM comparison of pronation/supination of stroke participants. In (a) and (b), P = pronation, S = supination. The wide and thin bars represent the mean values and individual results, respectively.

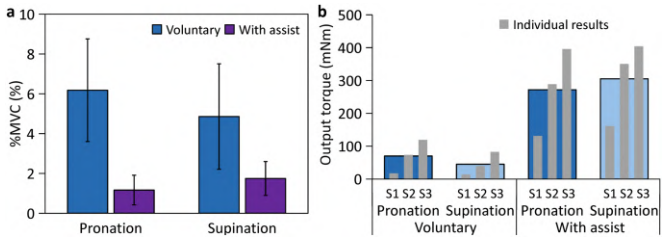

Fig. 10. Output torque evaluation. (a) Healthy participant test: %MVC measured at pronator teres (pronation) and biceps brachii (supination) for maintaining a 400 mNm moment with/without assist. The error bars indicate the standard error. (b) Stroke survivor test: Maximum voluntary torque with/without assistance. The wide and thin bars represent the mean values and individual results, respectively.

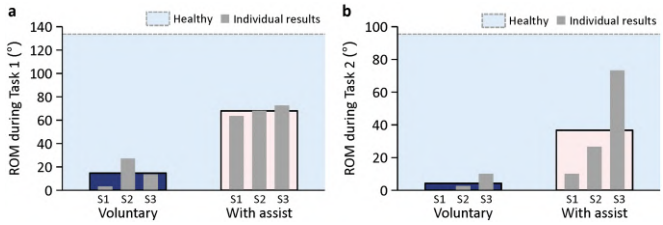

Fig. 11. ADL tasks evaluation. (a) ROM of stroke in bottle rotating task. (b) ROM of stroke in door opening task. The wide and thin bars represent the mean values and individual results, respectively. The shaded areas indicate the mean of healthy participants' performance in voluntary condition.

selected: 1) bottle (600 g) rotating task, and 2) door opening task (rotating doorknob to open door). Healthy participants were instructed to complete these tasks in voluntary condition. Stroke survivors were instructed to complete these tasks with and without the assistance from the device. Their performance was evaluated by measuring ROM during the task.

The wearability test consisted of donning and doffing the device without assistance from others. The participants were asked to practice using the device one time under guidance. Throughout the experiment, we emphasized to the participants that they should complete the task at a normal pace and not rush. In this way, participants were allowed to simulate the state of daily use of the skin-brace.

C. User Test Results

1) ROM Test: The ROM test results are depicted in Fig. 9(a) and (b). For healthy participants, the mean ± SE values of their forearm pronation and supination ROM were 78.2° ± 7.1° and 58.6° ± 15.5°, respectively, for voluntary condition, and 79.2° ± 5.7° and 57.1° ± 14.7°, respectively, with device-assistance. There was no significant difference between these two conditions for both pronation (paired t-test: $p = 0.438$) and supination (paired t-test: $p = 0.688$).

The ROM in the voluntary and with assistance condition from stroke survivors for pronation was 5.3° ± 4.8°and 43.9° ± 7.6°, respectively. For supination, the ROM was 14.1° ± 21.1° and 31.9° ± 8.7°, respectively: an increase of 828% and 226% for pronation and supination respectively. The passive ROM was measured by manual rotation of the participants' forearm in the pronation/supination direction until significant resistance was felt. The passive ROM were 54.2° ± 12.0° and 34.6° ± 9.7°, respectively. No significant difference was observed between the device-assisted condition and passive condition for both pronation (paired t-test: $p = 0.171$) and supination (paired t-test: $p = 0.387$).

2) Output Torque Test: As shown in the output torque test results (Fig. 10(a) and (b)), the muscle activation (%MVC) for healthy participants with device-assistance decreased to 1.17% ± 0.74% and 1.75% ± 0.85% from 6.18% ± 2.58% and 4.85% ± 2.65% compared with the voluntary condition at a 400 mNm output torque for pronation and supination, respectively. For all conditions, the output torque of stroke survivors was below the average output torque of the healthy participants with device assistance (452.7 ± 132.7 mNm), but in the condition of with assistance, the output torque of stroke survivors approached the output torque of healthy participants. The output torque in voluntary and with assistance condition from stroke survivors for pronation was 70.1 ± 51.2 mNm and 271.9 ± 133.3 mNm, respectively. For supination, the output torque was 45.1 ± 34.8 mNm and 305.2 ± 127.7 mNm, respectively. The output torque of pronation/supination of stroke survivors was improved by 388% and 676%, respectively, with assistance.

3) ADL Tasks Test: Fig. 11(a) and (b) shows the results of ADL tasks. The ROMs of healthy participants during bottle rotating and door opening tasks were 135.9° ± 7.1° and 96.0° ± 4.8°, respectively. For stroke survivors, the ROMs in unassisted and assisted conditions during task 1 were 14.7° ± 12.0° and 68.0° ± 4.5°, respectively. In task 2, the ROMs were 4.2° ± 5.2° and 36.7° ± 32.8°. Although ROMs in assisted condition were smaller than those of healthy due to the maximum assisting torque limit set for safety, stroke survivors could make enough ROM to conduct the tasks in assisted condition.

4) Wearability Test: The wearability test results are shown in Table III. Although stroke survivors, on average, took longer to don and doff the device than healthy participants (25.3 s ± 7.3 s and 13.9 s ± 5.3 s, respectively), the time for stroke survivors to don and doff the brace was significantly reduced to 47.1 s ± 15.3 s and 21.9 s ± 4.5 s (8th ˜ 10th trials) from 75.6 s ± 19.9 s and 54.3 s ± 21.1 s (first three trials), respectively.

TABLE III
DONNING AND DOFFING TIME

No.	Donning (*s*)		Doffing (*s*)	
	Beginning	Trained	Beginning	Trained
S1	98.3 ± 13.0	64.7 ± 7.4	54.2 ± 5.8	25.5 ± 4.4
S2	65.8 ± 6.8	36.6 ± 2.2	33.4 ± 7.0	16.8 ± 2.0
S3	62.2 ± 1.7	40.1 ± 3.3	75.4 ± 4.5	23.4 ± 3.4
Healthy (avg.)	25.3 ± 7.3		13.9 ± 5.3	

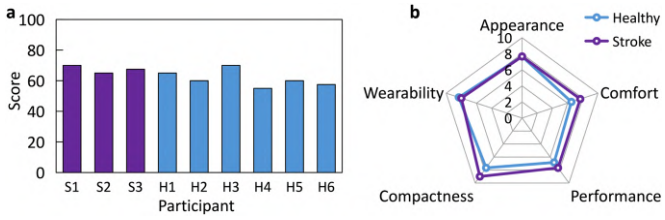

Fig. 12. Results of the user survey. (a) Scores from the standard SUS for all participants (b) Average scores from the custom questionnaire for healthy and stroke survivor participants.

5) Standard SUS and Customized Questionnaire: After performing the experiments, all participants were asked to fill a standard system usability scale (SUS), which is a quick, simple, and reliable tool for assessing the usability of a given system [25]. The average SUS score is 67.5 ± 2.5 for stroke survivors, and 61.3 ± 5.4 for healthy participants (Fig. 12(a)).

In addition, all participants also filled a customized questionnaire to quantify their subjective impression on the device. The results of all aspects are shown in Fig. 12(b). The questionnaire adopts a ten-point scale in regards to appearance (Stroke: 7.7 ± 1.2, Healthy: 7.7 ± 1.2), comfort (Stroke: 7.7 ± 1.2, Healthy: 6.5 ± 1.6), performance (Stroke: 7.7 ± 1.2, Healthy: 6.8 ± 1.0), compactness (Stroke: 9.0 ± 0.0, Healthy: 7.7 ± 1.2), and wearability (Stroke: 8.0 ± 1.0, Healthy: 8.3 ± 0.5). Stroke survivors gave slightly higher scores on the device than healthy participants. Furthermore, all participants could provide their feedback at the end of the experiments.

IV. Discussion and Conclusion

In this letter, we propose a compact and effective wearable skin-brace for assisting forearm pronation/supination movement in patients with neurological diseases hemiplegia. We adopted a lightweight and low-profile design for a skin-brace that can fit the forearm like clothing, while also ensuring a comfortable wearing experience and supporting individual customization. This skin-brace combines the advantages of a compact rail-tendon mechanism based on human anatomy and a soft tension transfer mechanism, which has high transfer efficiency and provides patients with compliance and sufficient assistance to complete everyday activities. A user-friendly design allows users to don and doff the brace independently in a quick and easy manner. With the advantage of not restricting other joint movements, the device also shows the potential of being used in conjunction with other rehabilitation devices.

Compactness is considered a high priority of our novel skin-brace. In existing forearm rehabilitation devices [5], [6], the rail is usually designed as a large and thick closed loop which is beyond the demand of the forearm ROM. Our proposed skin-brace enables the slider to complete a 150° rotation under the constraint of a 100° rail without restricting the movements of the hand and wrist. The hybrid structure design can provide rigidity against the pre-tightening force of the cables and non-axial moments without imposing pressure on joints, which is crucial for safe interaction of the device with the user. The weight and maximum thickness of the skin-brace are 133 g and 16 mm, respectively, which are significantly below recommended values suggested [17]. The brace is compact enough to be hidden under clothing and make no external visually perceptible difference when worn, which can be very positive for the psychosocial aspects of patients [26].

Previous studies shown that wearable devices with slightly mismatched sizes can lead to user discomfort and poor performance [12]. Our proposed parameter-correlated modeling algorithm and manufacturing process can provide each user with a low-cost and customized brace based on personal dimensions in a short time. This allows the skin-brace to fit the forearm and provide optimal assistance to the user.

Based on trajectory analysis of the kinematic motion of forearm pronation/supination, we propose a bio-adaptive spiral rail design, which can provide users with more comfortable assistance. Compared to the circular arc rail design, participants reported that they perceived less obstruction during forearm rotation with the brace based on bio-adaptive spiral rail design. We attribute this to the fact that the muscle-tendon models that contribute to forearm pronation/supination are inherently tilted towards radius and ulna rather than perpendicular to them. With the bio-adaptive rail-tendon actuating mechanism design, the tension vector of the cable is always highly aligned with the direction of the forearm rotation, regardless of the angular variations. Compared with similar pneumatic wearable devices [13], the proposed skin-brace can provide similar torque at different angles, with no singularity of insufficient power. During a cyclic test, the rail-tendon system achieved a durability of over 5,000 rotation cycles before the tendon broke due to wear and tear. The mechanism achieves a tension-to-torque ratio of 71% and is able to maintain a relatively constant transmission path length, minimizing slack, allowing bidirectional rotation of the forearm by single motor, which is a solid foundation for implementing a portable actuation system and ultimately reduces the size and inertia of the system, also lowers the required output torque from the motor.

The usability of the device was evaluated through user tests. The skin-brace can provide healthy participants with ROM assistance equivalent to what they could achieve in the voluntary condition. By comparing the differences in EMG signals, we verified that the device delays the onset of fatigue by reducing muscle activation in users when doing physical work with forearm movement. The abilities of stroke survivors, including both ROM and rotational torque, as well as their performance in ADL tasks, have received significant improvements with device assistance. The test results of stroke survivors also showed inter-individual variability, suggesting that the assistance users obtain from the skin-brace highly depends on their residual capacity and their joint stiffness.

In an unsupervised environment, donning/doffing a device is the first obstacle for patients to train independently [12]. The skin-brace allows users to independently don and doff the device in a short time (one minute to don, half a minute to doff), demonstrating excellent wearability. Even though it was challenging for stroke survivors at the beginning, they were able to dramatically reduce the time required after multiple practices, demonstrating a significant learning effect.

The overall usability of the skin-brace is fair as reflected by the SUS scores of healthy participants and stroke survivors, since an SUS score of 68 can be considered as average [27]. Both stroke survivors and healthy participants had a more positive impression in terms of the compactness and wearability of the skin-brace.

Future research should address the following issues. First, two healthy participants reported that they felt uncomfortable

pressure in their wrist area after prolonged wearing. However, for firm holding of the wrist, pressure on the skin in the contact area is unavoidable, we will revise the design by increasing contact area, different material selection, and choosing optimal thickness of the soft layer. Second, the current actuation unit is over the required specification needed for evaluating the performance of the skin-brace. However, based on the results of the tests, a more lightweight and compact actuation system is feasible and would eventually be designed as a fanny pack to allow the system to be fully wearable. Finally, future work may focus on the development of EMG-based control [28] for user intent recognition, and passivity analysis of the system.

REFERENCES

[1] T. Vos et al., "Global burden of 369 diseases and injuries in 204 countries and territories, 1990–2019: A systematic analysis for the global burden of disease study 2019," *Lancet*, vol. 396, no. 10258, pp. 1204–1222, 2020.

[2] M. Cianchetti, C. Laschi, A. Menciassi, and P. Dario, "Biomedical applications of soft robotics," *Nature Rev. Mater.*, vol. 3, no. 6, pp. 143–153, 2018.

[3] H. Manjunatha, S. Pareek, S. S. Jujjavarapu, M. Ghobadi, T. Kesavadas, and E. T. Esfahani, "Upper limb home-based robotic rehabilitation during COVID-19 outbreak," *Front. Robot. AI*, vol. 8, 2021, Art. no. 612834.

[4] M. J. Johnson, X. Feng, L. M. Johnson, and J. M. Winters, "Potential of a suite of robot/computer-assisted motivating systems for personalized, home-based, stroke rehabilitation," *J. Neuroeng. Rehabil.*, vol. 4, no. 1, pp. 1–17, 2007.

[5] E. Pezent, C. G. Rose, A. D. Deshpande, and M. K. O'Malley, "Design and characterization of the openwrist: A robotic wrist exoskeleton for coordinated hand-wrist rehabilitation," in *Proc. IEEE Int. Conf. Rehabil. Robot.*, 2017, pp. 720–725.

[6] H.-S. Park, Y. Ren, and L.-Q. Zhang, "Intelliarm: An exoskeleton for diagnosis and treatment of patients with neurological impairments," in *Proc. IEEE 2nd RAS EMBS Int. Conf. Biomed. Robot. Biomechatron.*, 2008, pp. 109–114.

[7] C. A. Yarosh, D. S. Hoffman, and P. L. Strick, "Deficits in movements of the wrist ipsilateral to a stroke in hemiparetic subjects," *J. Neuriophysiol.*, vol. 92, no. 6, pp. 3276–3285, 2004.

[8] K. K. Ang et al., "Brain-computer interface-based robotic end effector system for wrist and hand rehabilitation: Results of a three-armed randomized controlled trial for chronic stroke," *Front. Neuroeng.*, vol. 7, 2014, Art. no. 30.

[9] D. H. Kim, Y. Lee, and H.-S. Park, "Bioinspired high-degrees of freedom soft robotic glove for restoring versatile and comfortable manipulation," *Soft Robot.*, vol. 9, no. 4, pp. 734–744, 2022.

[10] T. Bützer, O. Lambercy, J. Arata, and R. Gassert, "Fully wearable actuated soft exoskeleton for grasping assistance in everyday activities," *Soft Robot.*, vol. 8, no. 2, pp. 128–143, 2021.

[11] C. G. Rose and M. K. O'Malley, "Hybrid rigid-soft hand exoskeleton to assist functional dexterity," *IEEE Robot. Automat. Lett.*, vol. 4, no. 1, pp. 73–80, Jan. 2018.

[12] C. Lambelet et al., "Characterization and wearability evaluation of a fully portable wrist exoskeleton for unsupervised training after stroke," *J. Neuroeng. Rehabil.*, vol. 17, no. 1, pp. 1–16, 2020.

[13] S.-H. Park, J. Yi, D. Kim, Y. Lee, H. S. Koo, and Y.-L. Park, "A lightweight, soft wearable sleeve for rehabilitation of forearm pronation and supination," in *Proc. IEEE 2nd Int. Conf. Soft Robot.*, 2019, pp. 636–641.

[14] P. C. LaStayo and M. J. Lee, "The forearm complex: Anatomy, biomechanics and clinical considerations," *J. Hand Ther.*, vol. 19, no. 2, pp. 137–145, 2006.

[15] K. D. Gordon, R. D. Pardo, J. A. Johnson, G. J. King, and T. A. Miller, "Electromyographic activity and strength during maximum isometric pronation and supination efforts in healthy adults," *J. Orthopaedic Res.*, vol. 22, no. 1, pp. 208–213, 2004.

[16] J. C. Perry, J. Rosen, and S. Burns, "Upper-limb powered exoskeleton design," *IEEE/ASME Trans. Mechatron.*, vol. 12, no. 4, pp. 408–417, Aug. 2007.

[17] Q. A. Boser, M. R. Dawson, J. S. Schofield, G. Y. Dziwenko, and J. S. Hebert, "Defining the design requirements for an assistive powered hand exoskeleton: A pilot explorative interview study and case series," *Prosthetics Orthotics Int.*, vol. 45, no. 2, pp. 161–169, 2020.

[18] S. Micera et al., "A simple robotic system for neurorehabilitation," *Auton. Robots*, vol. 19, no. 3, pp. 271–284, 2005.

[19] B. Radder et al., "User-centred input for a wearable soft-robotic glove supporting hand function in daily life," in *Proc. IEEE Int. Conf. Rehabil. Robot.*, 2015, pp. 502–507.

[20] S. Ozcakir, D. Sigirli, and H. Avsaroglu, "High wrist ratio is a risk factor for carpal tunnel syndrome," *Clin. Anatomy*, vol. 31, no. 5, pp. 698–701, 2018.

[21] M. S. Thiese et al., "Association between wrist ratio and carpal tunnel syndrome: Effect modification by body mass index," *Muscle Nerve*, vol. 56, no. 6, pp. 1047–1053, 2017.

[22] A. Schiele and F. C. Van Der Helm, "Kinematic design to improve ergonomics in human machine interaction," *IEEE Trans. Neural Syst. Rehabil. Eng.*, vol. 14, no. 4, pp. 456–469, Dec. 2006.

[23] S. J. Bae, S. H. Jang, J. P. Seo, and P. H. Chang, "The optimal speed for cortical activation of passive wrist movements performed by a rehabilitation robot: A functional nirs study," *Front. Hum. Neurosci.*, vol. 11, 2017, Art. no. 194.

[24] M. Knops et al., "Investigation of changes in body composition, metabolic profile and skeletal muscle functional capacity in ischemic stroke patients: The rationale and design of the body size in stroke study (bosss)," *J. Cachexia, Sarcopenia Muscle*, vol. 4, no. 3, pp. 199–207, 2013.

[25] A. Bangor, P. T. Kortum, and J. T. Miller, "An empirical evaluation of the system usability scale," *Int. J. Hum.–Comput. Interact.*, vol. 24, no. 6, pp. 574–594, 2008.

[26] I. Galiana, F. L. Hammond, R. D. Howe, and M. B. Popovic, "Wearable soft robotic device for post-stroke shoulder rehabilitation: Identifying misalignments," in *Proc. IEEE/RSJ Int. Conf. Intell. Robots Syst.*, 2012, pp. 317–322.

[27] J. Brooke, "SUS: A retrospective," *J. Usability Stud.*, vol. 8, no. 2, pp. 29–40, 2013.

[28] M. Oghogho, M. Sharifi, M. Vukadin, C. Chin, V. K. Mushahwar, and M. Tavakoli, "Deep reinforcement learning for emg-based control of assistance level in upper-limb exoskeletons," in *Proc. IEEE Int. Symp. Med. Robot.*, 2022, pp. 1–7.